

Nonblocking Monoclonal Antibody Targeting Soluble MIC Revamps Endogenous Innate and Adaptive Antitumor Responses and Eliminates Primary and Metastatic Tumors

Shengjun Lu¹, Jinyu Zhang¹, Dai Liu², Guangfu Li^{2,3}, Kevin F. Staveley-O'Carroll^{2,3}, Zihai Li^{1,3}, and Jennifer D. Wu^{1,3,4}

Abstract

Purpose: The human tumor-derived soluble MHC I-chain-related molecule (sMIC) is highly immune suppressive in cancer patients and correlates with poor prognosis. However, the therapeutic effect of targeting sMIC has not been determined, due to the limitation that mice do not express homologs of human MIC. This study is to evaluate the therapeutic effect of a monoclonal antibody (mAb) targeting sMIC in a clinically relevant transgenic animal model.

Experimental Design: We treated the engineered MIC-expressing "humanized" TRAMP/MIC bitransgenic mice at advanced disease stages with a sMIC-neutralizing nonblocking anti-MIC mAb and assessed the therapeutic efficacy and associated mechanisms.

Results: A sMIC-neutralizing nonblocking anti-MIC mAb effectively induced regression of primary tumors and eliminated

metastasis without inducing systemic toxicity. The therapeutic effect is conferred by revamping endogenous antitumor immune responses, exemplified by restoring natural killer (NK) cell homeostasis and function, enhancing susceptibility of MIC⁺-tumor cells to NK cell killing, reviving and sustaining antigen-specific CD8 T-cell responses, augmenting CD4 T cells to Th1 responses, priming dendritic cells for antigen presentation, and remodeling tumor microenvironment to be more immune reactive.

Conclusions: Therapy with a sMIC-neutralizing nonblocking anti-MIC mAb can effectuate antitumor immune responses against advanced MIC⁺ tumors. Our study provided strong rationale for translating sMIC-neutralizing therapeutic mAb into clinics, either alone or in combination with current ongoing standard immunotherapies. *Clin Cancer Res*; 21(21); 4819–30. ©2015 AACR.

Introduction

In response to oxidative stress and oncogenic insults, human epithelial cells were induced to express families of ligands for the immune stimulatory receptor NKG2D, presumably to provoke antitumor immune responses as a natural defense mechanism (1–4). In experimental animal models, ligand-induced activation of NKG2D has been demonstrated very effective in controlling tumor initiation and progression through activating natural killer (NK) and costimulating effector T cells, including cytotoxic T lymphocytes and NKT cells (5, 6). Notably, retaining surface NKG2D ligand expression has been shown to be critical for

NKG2D-mediated tumor suppression in both experimental animal models and cancer patients (7, 8). In cancer patients, however, tumors evolved to escape NKG2D-mediated natural immune response by adopting a protease or exosome-mediated strategy to shed NKG2D ligands (9). As a consequence, not only tumor cells lost surface NKG2D ligands with an impaired ability to provoke an effective immune response, but more severely, the shedding-resolved soluble NKG2D ligands can sabotage the immune system via diversified mechanisms. These include down-regulating the expression and thus function of the receptor NKG2D on NK cell and effector T cells (10, 11), perturb NK cell homeostasis (7), promoting the expansion of arginase 1⁺ myeloid-derived suppressor cells (MDSC), and skewing macrophage to the tumor-promoting alternatively activated phenotypes (12). Thus, tumor-derived soluble NKG2D ligands have been broadly accepted to be highly immune suppressive and proposed as a potential cancer immune therapeutic target (13, 14).

In human, two families of NKG2D ligands, the MHC I-chain-related molecules A and B (MICA/B, collectively termed MIC) and the HCMV glycoprotein UL16-binding protein family molecules (ULBP), have been identified; among which the MIC family is most prevalently and restrictedly expressed by human cancer cells (15). Shedding of tumor cell surface MIC to release the soluble MIC (sMIC) into circulation is commonly found in cancer patients (16–19). Serum levels of sMIC have been well associated with progressiveness of the diseases in multiple cancer types (7, 20–23). Given the multiple immune suppressive nature of

¹Department of Microbiology and Immunology, Medical University of South Carolina, Charleston, South Carolina. ²Department of Surgery, Medical University of South Carolina, Charleston, South Carolina. ³Cancer Immunology Program, Hollings Cancer Center, Charleston, South Carolina. ⁴Department of Medicine, University of Washington, Seattle, Washington.

Note: Supplementary data for this article are available at Clinical Cancer Research Online (<http://clincancerres.aacrjournals.org/>).

Corresponding Author: Jennifer D. Wu, Department of Microbiology and Immunology, Medical University of South Carolina, 86 Jonathan Lucas Street, Hollings Cancer Center 610, Charleston, SC 29425. Phone: 843-792-9222; Fax: 843-792-9588; E-mail: wujjd@musc.edu

doi: 10.1158/1078-0432.CCR-15-0845

©2015 American Association for Cancer Research.

Translational Relevance

The human tumor–derived soluble MHC I-chain–related molecule (sMIC) is highly immune suppressive in cancer patients and correlates with poor prognosis. However, whether sMIC is targetable for cancer therapy remains untested to date due to the lack of relevant preclinical models. Using an engineered MIC-expressing bitransgenic mouse spontaneous tumor model that closely recapitulates the onco-immune dynamics of human cancer, we demonstrate that therapy with a sMIC-neutralizing nonblocking anti-MIC monoclonal can effectuate remarkable antitumor responses to induce regression of primary tumors and eliminate metastasis. Our findings provide the first-in-field evidence conveying the therapeutic power of neutralizing sMIC and build the rationale to translate the therapy into clinics.

sMIC (7, 10, 12, 16), whether antibody neutralizing sMIC can revive host antitumor responses in MIC⁺ cancer patients is evidently an interesting therapeutic question. Because of the limitation that no MIC homolog is expressed by rodents, this critical question, however, remained unaddressed to date. Notably, although the signaling pathways of NKG2D are conserved across species, mouse NKG2D ligands differ from human MIC in their affinity, structure, regulation, and distribution in tumor tissues (15, 24, 25). These inherent differences preclude the translation of interesting biologic conclusions discovered from mouse NKG2D ligands to human cancer.

We have recently generated a "humanized" bitransgenic TRAMP/MIC(B) mouse model that expresses human MIC in the prostate epithelial cells of the SV40T-transgenic adenocarcinoma mouse prostate (TRAMP) directed by the prostate-specific promoter (7). The TRAMP/MIC mouse closely recapitulates the dynamic interaction of oncogenesis and NKG2D-mediated immune surveillance in human cancer patients by bridging shedding sMIC with disease progression (7). With close resemblance to MIC⁺ cancer patients (7, 17, 20, 21), high serum levels of sMIC in TRAMP/MIC mice predicted poor tumor prognosis (7). Utilizing this similarity, in this study, we evaluated the therapeutic antitumor efficacy of a sMIC-neutralizing but nonblocking anti-MIC monoclonal antibody (mAb) B10G5 in an immune tolerant spontaneous MIC⁺ tumor model.

Materials and Methods

Animals and antibody therapy

Breeding of TRAMP/MICB has been previously described (7). Animals were randomized into two cohorts receiving therapy with intraperitoneal (i.p.) injection of sMIC-specific mAb B10G5 or isotype control IgG (cIgG) at the dose of 4.0 mg/kg body weight twice weekly. Generation of the B10G5 antibody were described previously (7). All animals were treated for 8 weeks before euthanization that was designated as the study endpoint. Mice received daily refreshed drinking water containing 0.8 mg/mL bromodeoxyuridine (BrdUrd) for 5 consecutive days before the study endpoint. For congenic cells transfer, splenocytes were isolated from congenic CD45.1⁺ C57BL/6 mice (Charles River Laboratories, Frederick Cancer Research Center, Frederick, MD) and labeled with V₄₅₀ cell-trace dye

according to the manufacturer's protocol (eBioscience). V₄₅₀-labeled splenocytes were resuspended in PBS and injected via tail vein into recipient TRAMP/MICB mice (CD45.2⁺) at the dose of 2×10^7 /mouse 5 days before endpoint. All animals were housed in specific pathogen-free facilities. All experimental procedures were approved by the Institutional Animal Care and Use Committee. The study was repeated three times unless otherwise specified.

NK and CD8 T-cell depletion

Mice were injected with antibody anti-NKp46 antibody (BioLegend) to deplete NK cells or CD8 α -specific antibody (clone 53-6.7; BioXcell) to deplete CD8 T cells at the dose of 200 μ g/mouse 1 day before B10G5 antibody therapy and thereafter twice weekly at the dose of 100 μ g/mouse till study endpoint. Efficiency of depletion was confirmed by flow cytometry analyses in the peripheral blood.

Antigen-specific T-cell response experiment

CD8 T cells from TCR-I transgenic mice were labeled with CFSE and injected i.v. into animals (2×10^6 cells/mouse) that were receiving B10G5 or control IgG therapy. Animals were sacrificed at indicated time points to assess TCR-I T cell *in vivo* frequency with TCR-I-specific H-2D^b/TAG epitope I-tetramer (D^b/I-tetramer; ref. 26). To assay antigen-specific CD8 T-cell response, bulked splenocytes and single-cell suspension of tumor-draining lymph nodes (dLN) and tumor digests were stimulated overnight with 0.5 μ M TAG epitope I peptide and assaying intracellular IFN γ staining of CD8⁺ or D^b/I-tetramer⁺ T cells.

Tissue collection

Blood was collected via tail bleeding during therapy and via cardiac puncture after euthanization. Spleens and dLN were collected for immunologic analyses. Prostate, lung, liver, kidney, pancreas, and intestines were collected, fixed in 10% neutral fixation buffer followed by paraffin embedment or directly embedded in optimal cutting temperature (OCT), for pathologic and histologic analyses. In some experiments, partial of prostate tumors was digested with collagenase for analyses of tumor-infiltrated lymphocytes.

Flow cytometry

Single-cell suspension from splenocytes, dLN, or tumor infiltrates was prepared as described previously (7). Combination of the following antibody was used for cell surface or intracellular staining to define populations of NK, CD8, and subsets of CD4 T cells: CD3e (clone 145-2c11), CD8a (clone 53-6.7), CD4 (clone GK1.5), NK1.1 (clone PK136), NKG2D (clone CX5), CD45.1 (clone A20), and T-bet (clone eBio4B10). For *ex vivo* restimulation, single-cell suspension of freshly isolated splenocytes or LN were cultured in complete RPMI-1640 medium containing 50 ng/mL phorbol 12–myristate 13–acetate (PMA) and 500 ng/mL ionomycin for 4 hours and analyzed by intracellular staining with antibodies specific to IFN γ (XMG1.2). For NK cell renewal, intracellular BrdUrd staining was performed using anti-BrdUrd antibody (clone Bu20a). All antibodies and the corresponding isotype controls were fluorochrome conjugated and were purchased from eBioscience or BD Biosciences. Multicolored flow cytometry analyses were performed on an LSRII (BD). Data were analyzed with the FlowJo software (TreeStar).

Histology and immunohistochemistry staining

Prostate, lung, and other organs were sectioned and stained with H&E for histologic evaluation. For immunohistochemistry (IHC) staining to detect specific antigens, the following antibodies were used: anti-SV40T (Santa Cruz Biotechnology), anti-Ki67 (Neomarker), anti-cleaved Caspase-3 (Cell Signaling Technology; clone 5A1E), anti-CD8 (BD Biosciences), anti-NK1.1 (eBiosciences; PK136), and anti-synaptophysin (aBCAM). The IHC staining protocol has been previously described (7, 17). All tissues were counter stained with hemotoxyline for visualization of nucleus.

Serum sMIC, total IgG, and cytokine detection

Serum levels of sMICB and total IgG were assessed using respective Sandwich ELISA kit (R&D Systems). Serum levels of cytokines were assayed by Eve Technologies Corporation using the Luminex Technology.

Statistical analysis

All results are expressed as the mean \pm SEM. Mouse and sample group sizes were $n > 5$, unless otherwise indicated. Data were analyzed using unpaired *t* test, and differences were determined significant at $P < 0.05$. The Kaplan–Meier survival curves were generated using the GraphPad Prism software.

Results

Functional characterization of the anti-MIC mAb B10G5

The B10G5 mAb not only neutralizes free sMIC but also recognizes tumor cell surface membrane-bound MIC (Supplementary Fig. S1A and S1B), owing to sMIC sharing the same sequence and structure as the ectodomain of cell-surface MIC (16). Because B10G5 and the receptor NKG2D recognizes different epitopes of MIC (data not shown), B10G5 does not block the sensitivity of NKG2D-mediated NK cell cytolytic activity against MIC⁺ cells (Supplementary Fig. S1C). Conversely, B10G5 enhances the sensitivity of MIC⁺-tumor cells to NK cell cytotoxicity (Supplementary Fig. S1C), presumably through antibody-mediated cell cytotoxicity (ADCC) and/or enhanced immune synapse formation through simultaneously engaging NKG2D and Fc receptor on NK cells.

B10G5 antibody therapy effectively induced regression of primary tumors and eliminated metastasis

We have previously shown that TRAMP/MIC mice have greater than 40% incidence of developing highly invasive PD carcinoma and distant metastasis by 24-weeks of age (7). We also have previously determined that the accelerated tumor progression in TRAMP/MICB mice in comparison with TRAMP littermate is associated with elevated serum sMIC and its immune suppressive effects as in cancer patients with advanced diseases (7, 20, 21, 23, 27). With the specific aim to treat advanced cancer, we treated random cohorts of 27- to 28-week-old TRAMP/MIC mice with the B10G5 mAb or control mouse IgG (cIgG) twice weekly via i.p. route at the dose of 4 mg/kg body weight (Fig. 1A). Following an 8-week therapy, all mice that received B10G5 survived, whereas approximately 50% of mice in the control group, succumbed to the disease during the same time frame with the remaining of mice showing severe symptoms of illness (Fig 1B–E and data not shown). Mice that received the 8-week B10G5 therapy had significantly smaller prostate tumor mass in comparison with those having received cIgG or to those at the same disease stage when

treatment began (27–28 week old; Fig. 1C and D). No metastasis was found in the B10G5-treated mice. Conversely, over 90% of the mice receiving cIgG developed metastasis (Fig. 1E). Systemically, in response to B10G5 therapy, serum levels of sMIC were significantly reduced (Fig. 1F).

A remarkable serum cytokine and chemokine "storm" that was likely elicited by multitude activation of cellular immunity was evident after the 8-week B10G5 therapy (Fig. 1G), as the "storm" was negatively influenced by depletion of respective specific lymphocyte subset during therapy (Supplementary Fig. S2). The "storm" exhibited marked elevation of major antitumor cytokines and immune activation chemokines, for example, IFN γ , IL2, IL12, IL9, and CCL5. No cytokine storm was elicited in TRAMP/MICB mice at any other age or tumor development stages or in non-tumor-bearing TRAMP/MICB.A2 mice (ref. 7; data not shown), suggesting that the "storm" is therapy induced. Notably yet, no significant systemic toxicities, such as body weight loss, increase in serum IgG, or C-reactive protein (CRP) or inflammation in other organs (liver, kidney, intestinal, and pancreas) were observed in response to B10G5 therapy (Fig. 1H and J and data not shown).

Therapy eliminates invasive prostate tumor cells and primes tumor microenvironment to be more immune reactive

Histologic examination revealed that animals having received B10G5 therapy exhibited a mixture of normal prostate gland and organ-defined well-differentiated prostate carcinoma, whereas mice having received cIgG therapy exhibited high frequency of invasive prostate carcinoma (Fig. 2A). B10G5 therapy resulted in markedly reduced proliferation (Ki67⁺) and increased apoptosis (C-caspase⁺) of carcinoma cells (Fig. 2A). In the primary tumor of majority TRAMP/MIC mice receiving cIgG or no therapy, a distinct population of disseminated tumor cells that gained neuroendocrine differentiation marker synaptophysin was abundantly present in the stroma (SYN; Fig. 2A). Clinically, these tumor cell types were considered to be therapy-resistant and confer a poor prognosis (28, 29). B10G5 therapy effectively eliminated the "neuroendocrine-differentiated" tumor cells.

In most solid tumor of human cancers, tumor infiltration of NK cells correlated with better clinical outcomes or better response to therapy (30–34), suggesting an important role of NK cell in controlling cancer progression. Resembling human cancer, we have recently shown that NK cell is rarely found in poorly differentiated prostate carcinoma (7). B10G5 therapy evidently enriched NK cell infiltration in the prostate tumor parenchyma (NKp46; Fig. 2B). Moreover, CD8 T-cell infiltration to tumor parenchyma was also enriched by B10G5 therapy (CD8; Fig. 2C).

We have recently shown that sMIC can facilitate the expansion of MDSC and skew macrophage into the arginase I⁺ alternatively activated phenotypes (12). Consistently, TRAMP/MIC had rich infiltration of arginase I⁺ cells in the prostate infiltrates, which were eliminated significantly by B10G5 therapy (arginase I; Fig. 2B). As arginase I can be produced by MDSC (generally defined as CD11b⁺Gr-1⁺) and/or the alternatively activated tumor-associated macrophage (generally defined as CD206⁺CD11c⁻; refs. 35–38), we further defined these immune suppressive subsets in tumor infiltrates by flow cytometry analyses. The numbers of CD11b⁺Gr-1⁺ MDSC and CD206⁺CD11c⁻ macrophages are both significantly decreased in response to B10G5 therapy (Fig. 2C and D). Together, these data demonstrate that neutralizing sMIC primed tumor microenvironment to be more immune active.

Lu et al.

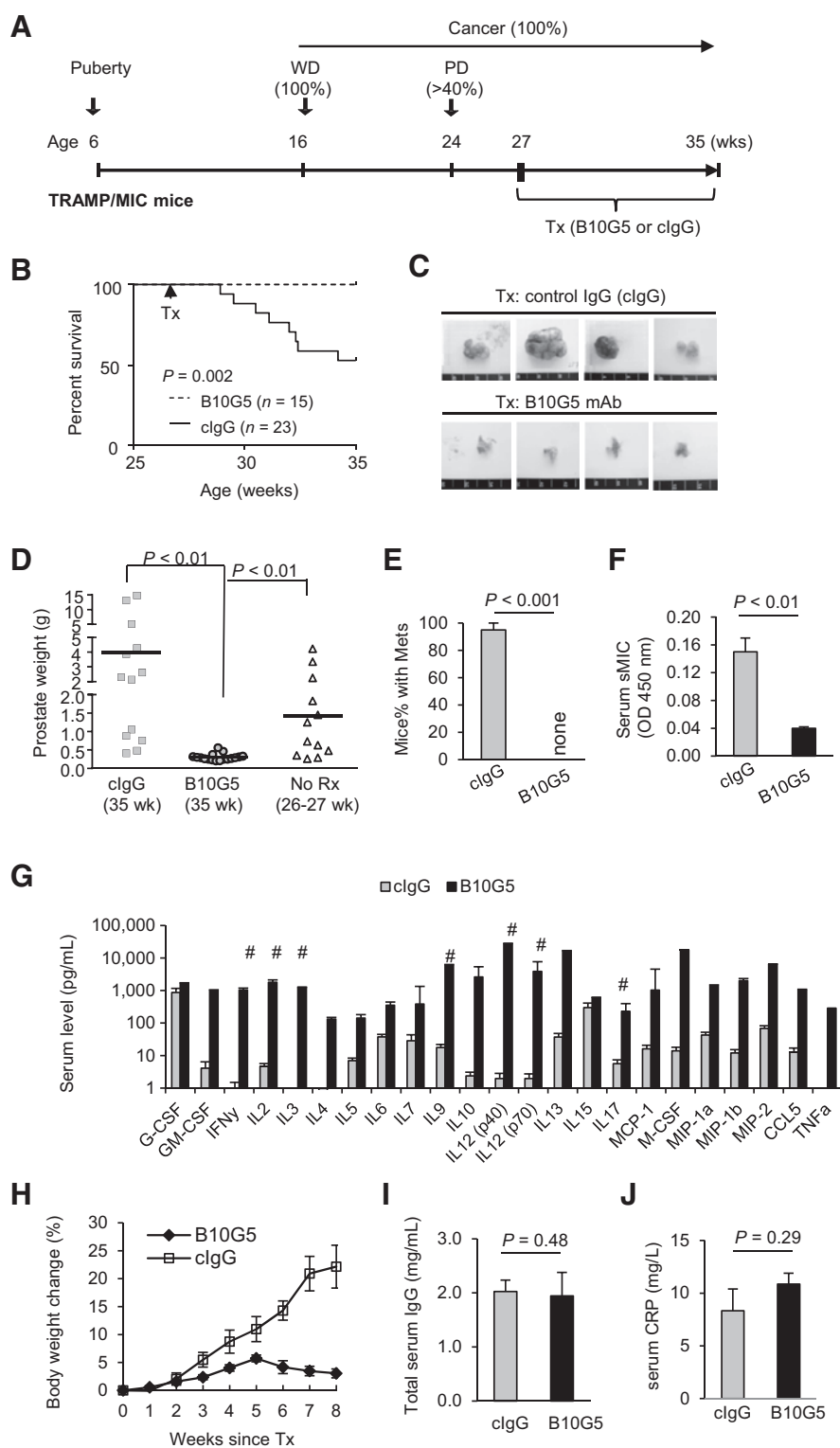


Figure 1.

sMIC-specific mAb B10G5 is highly effective against primary prostate carcinoma and metastasis in the double transgenic TRAMP/MIC mice. A, depiction of treatment. TRAMP/MIC mice received 4.0 mg/kg body weight of anti-sMIC mAb B10G5 therapy or control IgG (clgG) starting at 27-weeks old. Therapy was given twice weekly for 8 weeks. B, cumulative survival curve of mice receiving B10G5 therapy or control IgG. Data are combined from four independent therapy experiments. C, representative gross prostate size from mice receiving B10G5 therapy or clgG at the study endpoint. D, summary of prostate weight (tumor) from animals receiving B10G5 therapy in comparison with those from animals receiving clgG in parallel studies or to those from mice at the same age as therapy initiation (26–27 weeks). E, summary of metastatic incidence. F, B10G5 therapy reduces serum levels of sMIC measured by sandwich ELISA. G, levels of serum cytokines in response to therapy. Note that the Y-axis is in log-scale. Cytokine concentration was measured by Eves Technology Inc. with cytokine multiplex assay. # indicates measure immune stimulatory cytokines. H, whole body weight change of mice over the treatment course. Because of large primary tumor burden, an increase in body weight was observed in animals receiving clgG. I, levels of serum total IgG level at the study endpoint. J, levels of serum CRP at the study endpoint.

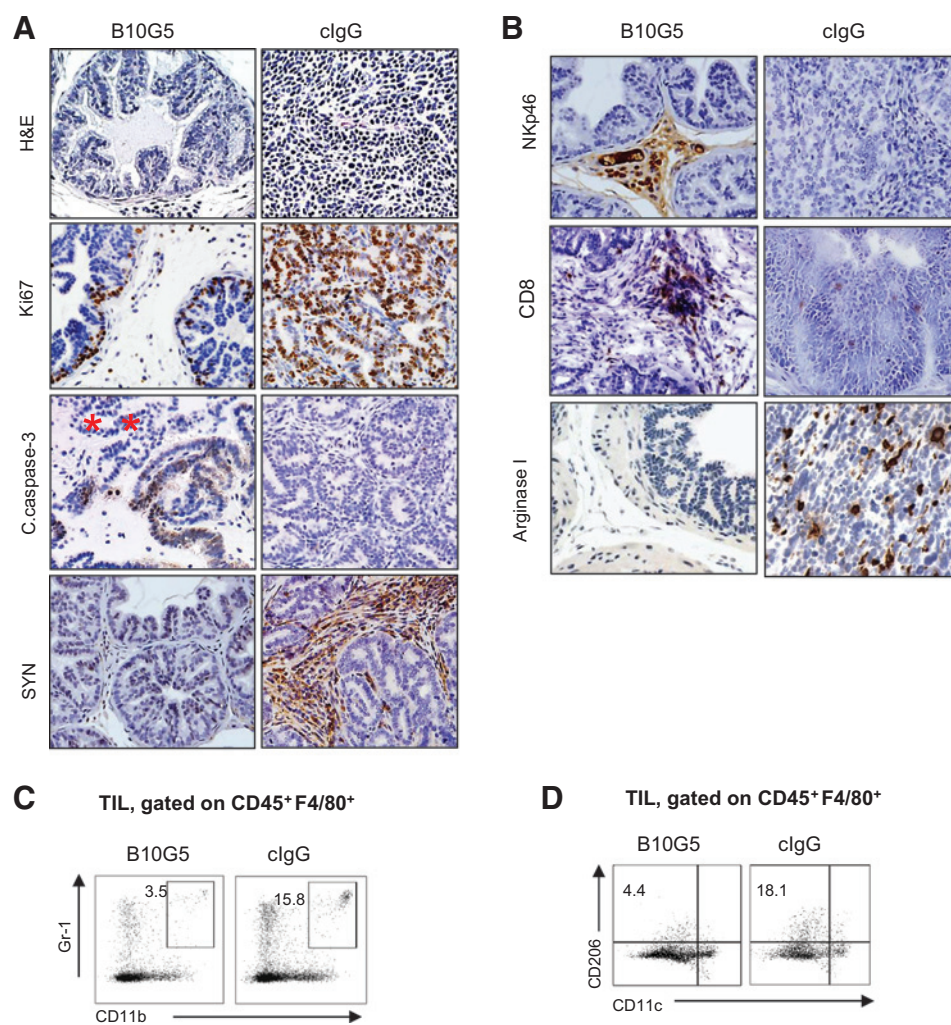
B10G5 therapy restores NK cell homeostasis and enhances NK and NKT cell function

Elevated serum sMIC was shown to impair peripheral NK cell function in cancer patients at large through downregulating NKG2D expression and reducing the number of NK cells

(7, 17, 18, 39). With the clinically relevant TRAMP/MIC mouse model, we demonstrated that high levels of sMIC ablates the ability of NK cells to self-renew (7). B10G5 therapy remarkably restored NK cell pool in the periphery and the ability of NK cell homeostatic to self-renew as evidenced by BrdUrd uptake after a

Figure 2.

B10G5 therapy inhibits primary tumor proliferation and survival, eliminates disseminated malignant tumor cells, and remodels prostate tumor microenvironment. A, representative micrographs demonstrating that B10G5 therapy inhibits prostate cancer cell proliferation (Ki-67⁺), induces tumor cell apoptosis (C-caspase 3⁺), eliminates malignant disseminated neuroendocrine tumor cells from the stroma (SYN⁺). B, representative micrographs demonstrating that B10G5 therapy increases immune active NK (NKP46⁺) and CD8 T cells and decreases arginase 1⁺ immune suppressive cells in tumor infiltrates. C, representative flow cytometry analyses of MDSC defined by Gr-1⁺CD11b⁺ in tumor infiltrates. D, representative flow cytometry analyses of alternatively activated macrophages defined by CD206⁺CD11c⁻ in tumor infiltrates.



consecutive 5-day BrdUrd pulsing (Fig. 3A–D). Moreover, B10G5 therapy markedly enhanced NK cell function, illustrated by increased production of IFN γ in response to mitogen stimulation and cytolytic ability against NKG2D ligand-positive target cells (Fig. 3E–G). Together, these data conclude that targeting serum sMIC significantly restores NK cell homeostatic maintenance and function in MIC⁺ cancer host. The conclusion was further supported by adoptively transfer experiments with V₄₅₀-labeled CD45.1 congenic NK cells to B10G5 or clgG-treated TRAMP/MIC mice (Supplementary Fig. S3). Furthermore, although B10G5 therapy did not significantly affect the pool of NKT cells (data not shown); however, therapy enhanced Th1-like functional potential of NKT cells as represented by significantly increased IFN γ production in response to PMA/I stimulation (Fig. 3H and I).

B10G5 therapy potentiated CD8 and CD4 T cells antitumor responses

Tumor-derived sMIC has been shown to downregulate NKG2D expression on CD8 T cells in cancer patients (16). NKG2D, as a T-cell costimulatory receptor, is expressed by all human CD8 T cells but only by activated mouse CD8 T cells (4). B10G5 therapy in TRAMP/MIC mice significantly increased the population and

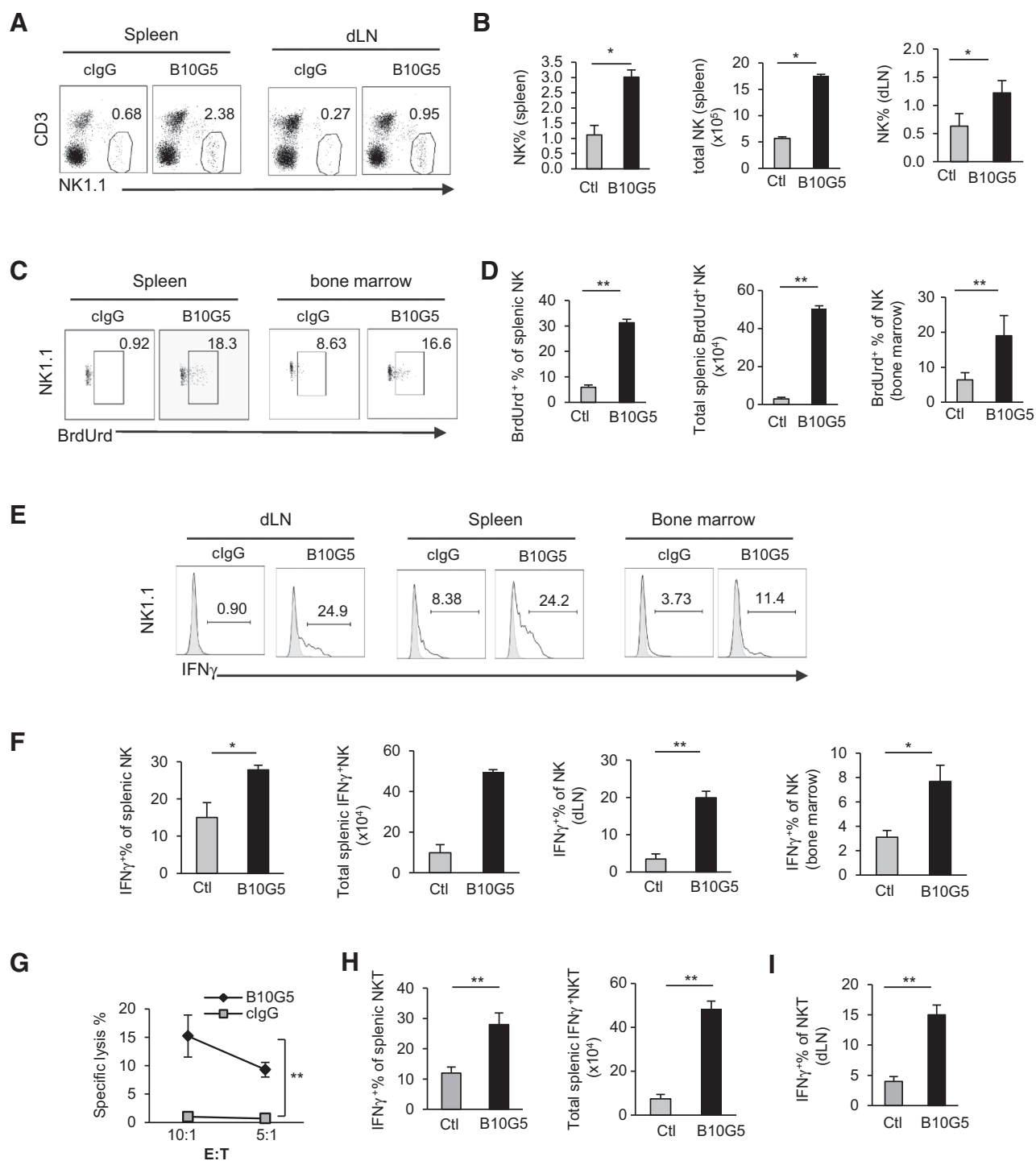
number of NKG2D⁺ CD8 T cells in the periphery (Fig 4A and B), indicating activation of CD8 T cells. When stimulated *ex vivo* with mitogen, CD8 T cells from mice receiving B10G5 therapy had significantly higher frequency and magnitude of IFN γ production (Fig. 4C and D). Moreover, B10G5 therapy significantly increased the number of CD8 T cells with CD44^{hi} memory phenotype in the spleen, tumor-dLN, and tumor infiltrates (Fig. 4E and F). Given that anergy and lack of trafficking to tumor sites are the major mechanisms of cytotoxic T dysfunction in most cancer types, these data suggest that targeting sMIC can effectively revive cytotoxic CD8 T-cell antitumor response in cancer host.

NKG2D is rarely expressed by CD4 T cells. However, B10G5 therapy potentiated CD4 T cells to Th1 responses in the tumor dLNs, shown by the significant increases in IFN γ ⁺ CD4 T cells in response to mitogenic stimulation (Fig 4G and H) and increases in T-bet expression (Supplementary Fig. S4). Furthermore, therapy also resulted in significant increase in CD4 T cells with CD44^{hi} memory phenotype (Fig 4I).

Therapy breaks CD8 T-cell tumor antigenic tolerance and augments antigen-specific responses

Male TRAMP mice express the SV40-T-Antigen (TA_g) oncoprotein specifically in the prostate to drive spontaneous

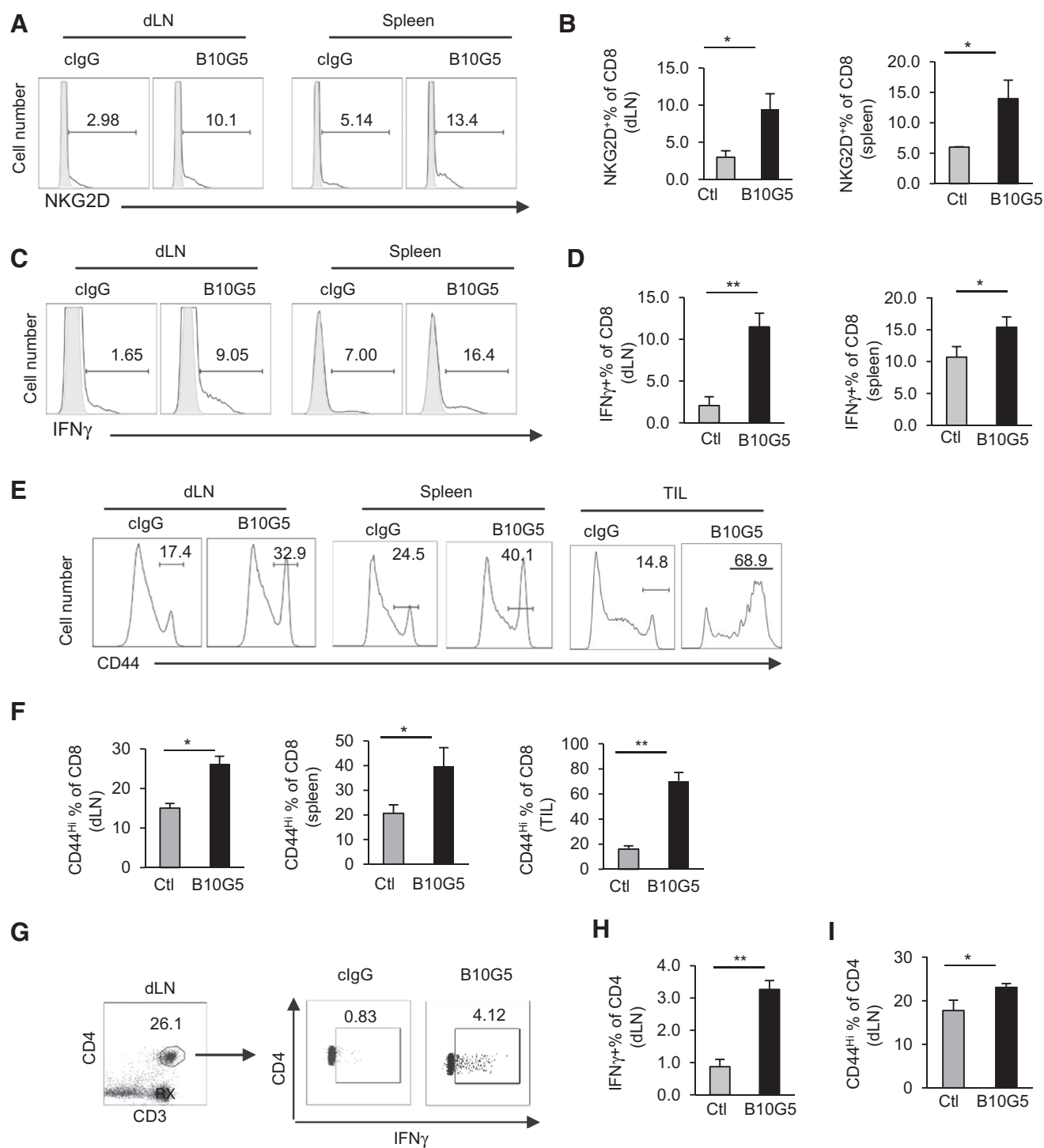
Lu et al.

**Figure 3.**

B10G5 therapy in TRAMP/MIC mice enhances NK cell homeostatic maintenance and function. A and B, B10G5 therapy significantly increased the number of NK cells in the periphery. C and D, B10G5 therapy significantly enhanced NK cell renewal as shown by the increase in the number of NK cells that are BrdUrd⁺ after 5-day labeling. E and F, B10G5 therapy significantly enhanced NK cell IFN γ production in response to PMA/ionomycin stimulation. G, splenic NK cell cytotoxicity against NKG2D-L⁺ RMA-S-Rae-1-positive cells. E:T = effector:target. H and I, B10G5 therapy increases NKT population and functional potential shown by IFN γ production in response to PMA/I stimulation. *, $P < 0.05$; **, $P < 0.01$.

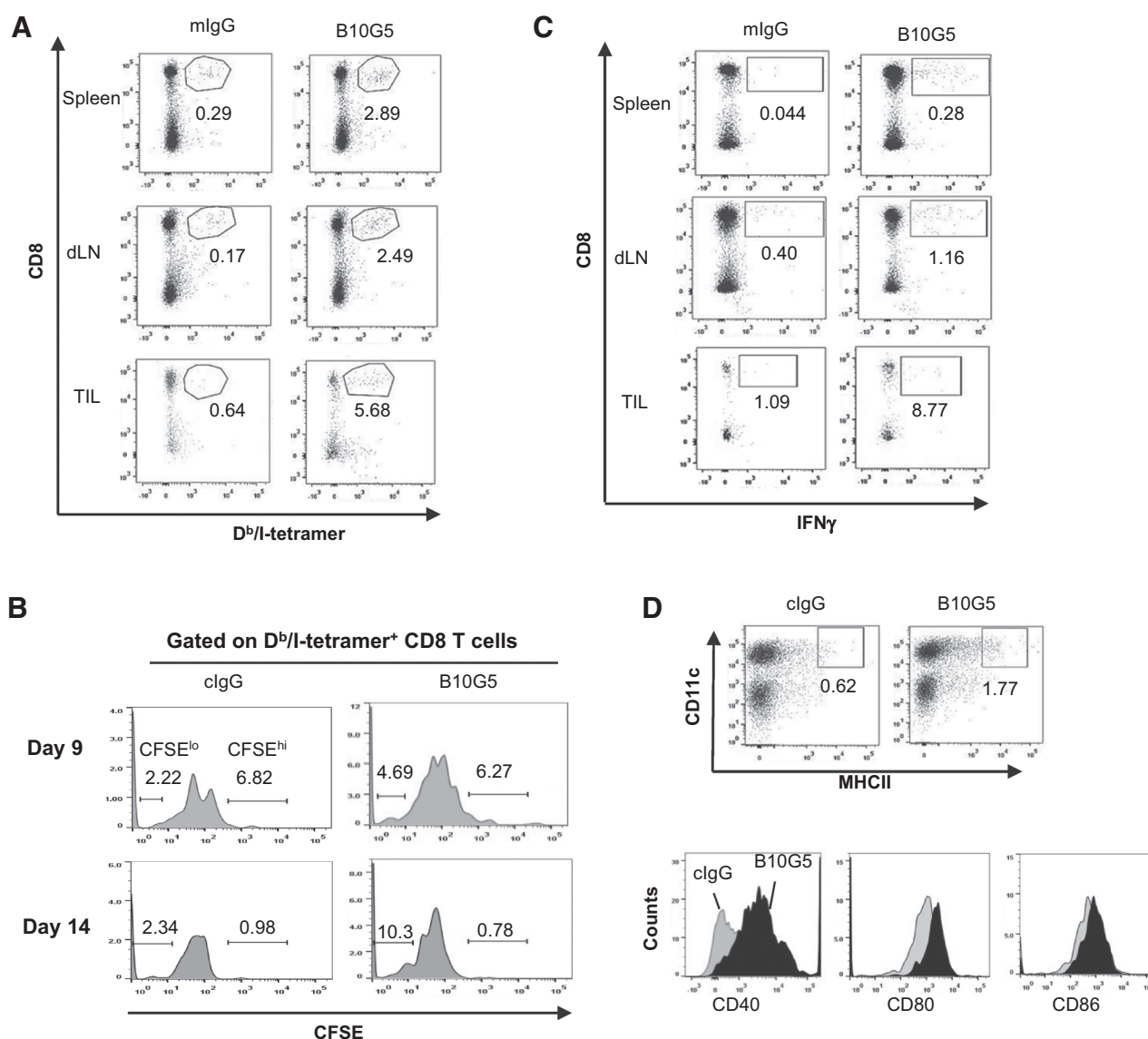
prostate tumor development through inactivation of tumor suppressor genes p53 and Rb pathways (40). Akin to the biology in cancer patients, the TAGs in male TRAMP mice

serves as a self-antigen and a tumor antigen, leading to tolerance of TAG and clonal deletion of TAG-specific T cells (41). Adoptively transferred naïve CD8 T cells that bear TAG-specific

**Figure 4.**

B10G5 therapy in TRAMP/MIC mice potentiates CD8 and CD4 T cell antitumor function. A and B, representative flow cytometry plots (A) and summary statistics (B) demonstrating that B10G5 therapy significantly increases the expression of the costimulatory NKG2D on CD8 T cells, an indication of CD8 T-cell activation in mouse. C and D, representative flow cytometry plots (C) and summary statistics (D) demonstrating B10G5 therapy potentiates the CD8 T-cell IFN γ production in response to *ex vivo* restimulation by PMA and ionomycin. E and F, representative flow cytometry CD8 T cells with CD44^{hi} memory-phenotype. G and H, representative plot of flow cytometry and summary data demonstrating Th1 polarization of CD4 T cells in tumor-dLN. I, summary data demonstrating that B10G5 therapy increases CD44^{hi} memory phenotype of CD4 T cells in tumor-dLN. Data are representatives of three independent studies. $n > 5$ for animals in each group. *, $P < 0.05$; **, $P < 0.01$.

Lu et al.

**Figure 5.**

B10G5 therapy breaks tumor antigen-specific CD8 T-cell tolerance. CFSE-labeled TCR-I CD8 T cells bearing TCR specific for H-2D^b-restricted TAg epitope I were adoptively transferred into cohorts of TRAMP/MICB mice ($n = 5-7$, 2×10^6 cells/mouse) receiving therapy with B10G5 or clgG. Mice were euthanized at days 9 and 14 after transfer for analyses. Because of lack of endogenous CD8 T cells specific for TAg epitope I, adoptively transferred TCR-I-specific CD8 T cells were identified by positive staining for H-2D^b-TAg-epitope I tetramer (D^b/I-tetramer). A, representative dot plots demonstrating frequency of D^b/I-tetramer⁺ CD8 T cells in the spleen, tumor-dLN and tumor infiltrates at day 9 after transfer. B, representative dot plots demonstrating proliferation of D^b/I-tetramer⁺ CD8 T cells at days 9 and 14 after transfer. C, CD8 T cell IFN γ production in response to TAg epitope I stimulation. A total of 1×10^6 bulked splenocytes and single-cell suspension from tumor-dLN were stimulated with 0.5 μ mol/L of TAg 206-215 epitope I overnight. IFN γ production was assessed by intracellular staining. D, expression of DC activation markers in tumor-dLN (day 14). Gray fill profile, mice received clgG treatment. Black filled profile, mice received B10G5 treatment.

TCR became rapidly tolerant in TRAMP mice after initiation expansion (42).

We sought to address whether anti-sMIC antibody B10G5 therapy can enhance antigen-specific CD8 T-cell responses in TRAMP/MIC mice. Because of the clonal deletion of TAg-specific CD8 T cells (41), we thus adoptively transferred CFSE-labeled naïve CD8 T cells from the TCR-I mice that express a transgenic TCR recognizing H-2D^b-restricted epitope I of the TAg (residues 206-215; ref. 26). As examined at day 9 after transfer, a significantly higher number of H-2D^b/epitope I-specific tetra-

mer (D^b/I-tetramer) positive CD8 T cells was detected in the spleen, tumor-dLN, and tumor infiltrates of mice receiving B10G5 therapy than those receiving clgG therapy (Fig. 5A). Notably, endogenous D^b/I-tetramer⁺ CD8 T cells were not detectable in TRAMP/MIC mice with or without antibody treatment (Supplementary Fig. S5). The D^b/I-tetramer⁺ CD8 T cells are thus originated from adoptively transferred TCR-I cells. Consistent with findings in other studies (26, 43), adoptively transferred naïve TCR-I CD8 T cells (identified by D^b/I-tetramer⁺) underwent initial rapid expansion in all mice

as shown by low percentage of CFSE^{hi} tetramers when examined at day 9 (Fig. 5B), owing to encountering TAG. However, TCR-I CD8 T cells only continued to expand in mice receiving B10G5 therapy, as shown by marked increase in the percentage of D^b/I-tetramer⁺CFSE^{lo} cells when examined at day 14 after transfer (Fig. 5B). We further tested antigen-specific responsiveness of CD8 T cells by stimulating single-cell suspension from bulked splenocytes, tumor-dLN, or tumor digests with TAG epitope I peptide. As shown in Fig. 5C, B10G5 therapy markedly enhanced the capacity of CD8 T cells to produce IFN γ in response to TAG-specific epitope I peptide (TAg 206-215) stimulation.

In vitro studies have elegantly demonstrated that MIC⁺-tumor cells coated with anti-MIC antibody can opsonize dendritic cells (DC) and enhance antigen cross-presenting to CD8 T cells (44, 45). We thus further investigated whether this mechanism may contribute, at least in part, to the enhanced antigen-specific TCR-I T cells expansion and responses in the current experiment settings. As representatively shown in Fig. 5D, B10G5 therapy not only enriched mature DC presence in tumor-dLN not only marked elevated the expression of DC surface activation molecule CD40 and costimulatory molecule CD80/86. Altogether, these data evidently demonstrated that mAb targeting serum sMIC can effectively overcome tumor antigen-specific CD8 T-cell tolerance and enhance DC priming for antigen-presentation.

Our data in the clinically relevant TRAMP/MIC mouse have demonstrated that B10G5 neutralizing sMIC can effectively provoke a multitude of immune responses to suppress tumor growth and metastasis. We further substantiated these findings with experiments demonstrating that B10G5 effectively retarded the growth of transplantable TRAMP-C2 prostate tumor cell lines that express sMICB (TC2-sMICB) using the syngeneic MICB transgenic mouse model (Supplementary Figs. S6 and S7).

As tumors can be highly heterogeneous in differentiation and surface MIC retention, we further investigated the therapeutic effect of B10G5 against tumors expressing surface MIC. We treated cohorts of TRAMP/MICB mice of 20 weeks of age, at which time most of the tumors are well-differentiated and retained surface MIC expression as we have shown previously (7). A significant therapeutic response was also achieved although host immune responses were amplified at discrete magnitudes (Supplementary Fig. S8), presumably due to dissimilar mechanisms to which conferred by neutralizing sMIC.

Therapeutic antitumor effect is conferred by NK and CD8 T cells and CD4 Th1 response is NK-dependent

To this end, our data have suggested that therapy with a mAb B10G5 targeting sMIC effectively induces regression of advanced MIC⁺ malignancies through restoring innate and adaptive antitumor responses. We further address the contribution of NK and CD8 T cells in conferring the therapeutic effect of B10G5. Depleting NK or CD8 T cells in TRAMP/MICB mice during B10G5 therapy significantly mitigated the therapeutic effect of B10G5 (Fig. 6), exemplified by a significantly higher number of animals succumbed to tumor-related death, owing to larger primary tumor burden and/or development of lung metastasis (Fig. 6A–C). Depletion of CD4 T cells did not present a significant impact on therapeutic effect of B10G5 (data not shown). Because of the functional heterogeneity of multiple CD4 T cells subsets, the outcome is somewhat anticipated.

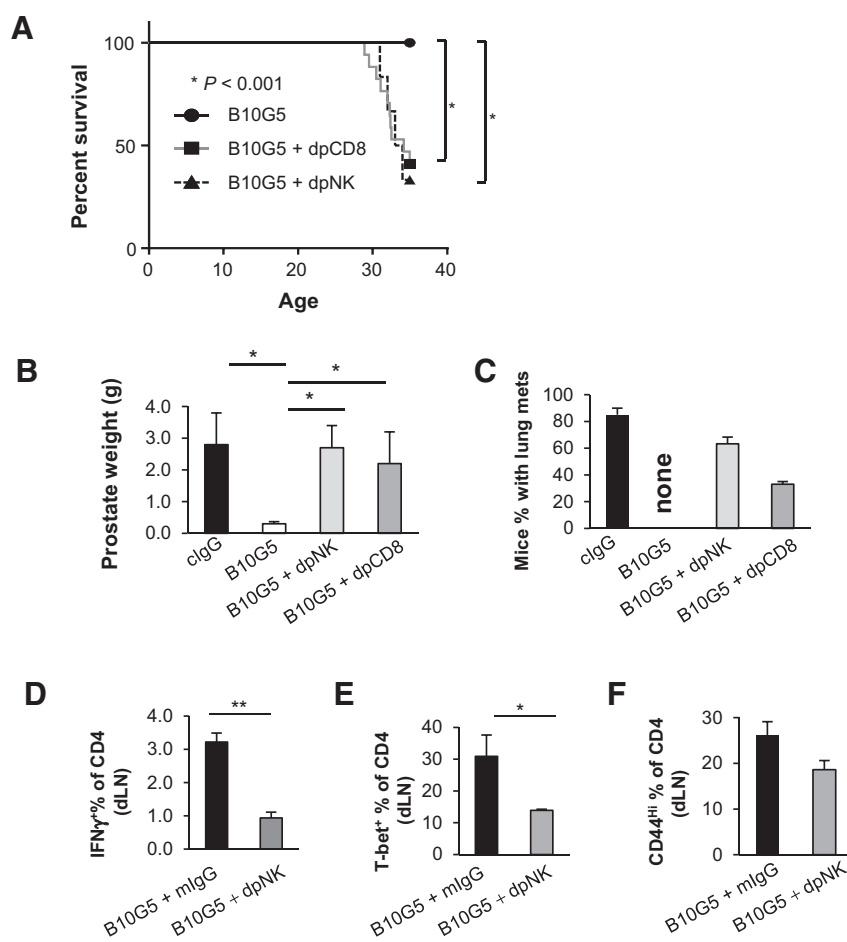
Intriguingly, with depletion of NK cells, B10G5 therapy failed to evoke CD4 T cells to generate optimal Th1 immune responses and maintaining CD44^{hi} memory phenotypes (Fig. 6D–F and Supplementary Fig. S9). Depletion of CD8 T cells had nominal effect on CD4 T cells (data not shown). These data not only suggest that both NK and CD8 T cells are required to generate optimal antitumor responses, but also suggest that functional NK cells are essential for generating optimal CD4 T-cell responses.

Discussion

Tumor-derived sMIC, whether through protease-mediated shedding or exosome secretion, has been shown to be highly immune suppressive in cancer patients through multiple mechanisms (9, 10, 46). However, whether a therapy targeting sMIC can revitalize host endogenous immune response remains untested. Using a clinically relevant double transgenic TRAMP/MIC mouse model that closely recapitulates the dynamics of serum sMIC and tumor progression, here we demonstrate that therapy with a nonblocking anti-MIC mAb to neutralize serum sMIC effectively induce regression of advanced primary tumors and eliminated metastasis through revamping host endogenous innate and adoptive antitumor immune responses and remodeling tumor micro-environment. Therapy effectuated endogenous antitumor responses by recuperating the ability of NK cells to self-renew and to be tumor-destructive, enhancing antigen-specific CD8 T-cell antitumor responses, and potentiating CD4 T cells to Th1 responses. Not only so, therapy also remodels tumor microenvironment demonstrated by enhancing tumor infiltration of NK cells and cytotoxic CD8 T cells and eliminating arginase I⁺ immune suppressive myeloid cells in tumor parenchyma. Remarkably, therapy elicited a systemic cytokine "storm" including major antitumor cytokines, without inducing systemic auto-immune cytotoxicity. Our study has provided the compelling first-in-field preclinical evidence that therapy with a sMIC-neutralizing nonblocking anti-MIC mAb alone can obliterate immune suppressive effective of tumor-derived sMIC and revive endogenous antitumor immune responses. Our findings define a new effective and feasible translational approach for cancer immunotherapy.

During oncogenesis, whether due to mutations in tumor suppressor genes or oncogenes, cells undergo aberrant DNA replication which initiates DNA repair responses as the cellular check point. This DNA repair response also triggers systemic checkpoint by upregulating NKG2D ligand, predominantly MIC, expression to alert the immune system to eliminate abnormal cells (1, 3). However, this oncoimmunologic coevolutionary process eventually renders tumor immune escape of NKG2D-mediated immune surveillance and allows tumors to progress. Proteolytic proteases or exosome-mediated tumor-shedding of sMIC accounted for one of the major mechanisms for MIC⁺ tumor evasion of NKG2D immune surveillance (9, 10, 46). Earlier studies demonstrated that sMIC induced global NKG2D downmodulation on all subsets of antitumor effector cells, such as CD8, NK, NKT, and $\gamma\delta$ T cells, in cancer patients (10, 11, 46). Recent studies have further demonstrated that sMIC can produce more profound immune suppressive effect by perturbing NK cell homeostatic maintenance and facilitating the expansion of arginase I⁺ myeloid suppressor cells (7, 12). These studies endorsed the viability of blocking sMIC pathways in cancer immunotherapy.

Lu et al.

**Figure 6.**

Affect of NK and CD8 T cells during B10G5 therapy. Data were obtained from cohorts ($n = 5-8$) of TRAMP/MIC mice that received i.p. injection with either 4 mg per kg body weight (mg/kg) B10G5 therapy alone twice weekly or in combination with 8 mg per kg body weight (mg/kg) anti-NKp46 antibody (BioLegend) to deplete NK cells or anti-CD8 α (Cedarlane Laboratories) to deplete CD8 T cells starting at the age of 27 weeks for 8 consecutive weeks. All mice were sacrificed at the age of 35 weeks if not died of tumor burden. A, a Kaplan-Meier plot showing overall survival rate. B, prostate weight (g) collected at sacrifice. C, percentage of mice with metastasis at necropsy. D, IFN γ production of CD4 T cells from tumor-dLN in response to PMA/ionomycin restimulation. E, T-bet expression in CD4 T cells from tumor-dLN. F, memory phenotype CD44^{hi} CD4 T-cell population in tumor-dLN.

How to feasibly target the immune suppressive effect of sMIC to translate into clinics is a critical question. Strategies has been proposed to blocking MIC shedding through targeting enzymes that regulates MIC shedding, such as the disulfide isomerase ERp5 (47, 48), ADAM 10/17 (49), and MMPs (50). These strategies are likely work well in early stage of diseases to retain maximal surface MIC expression and to preserve NKG2D-mediated antitumor immunity. In advanced cancer patients, however, providing that tumor cells lost surface MIC expression at large as a result of shedding and that endogenous immune responses have been severely sabotaged by high serum levels of sMIC through multiple mechanisms, strategy to prevent MIC shedding is likely to elicit nominal therapeutic effect. Under this scenario, neutralizing serum sMIC with mAb would be the logical approach in advanced cancer patients to alleviate the immune suppressive effect. Jinushi and colleagues (22, 45) reported that patients who developed high titer of serum levels of anti-MIC autoantibody during clinical trial with CTLA-4 blockade and/or vaccine therapy had sustained clinical response. These clinical findings strongly support the translational potential of our study and our unique sMIC-neutralizing nonblocking anti-MIC mAb.

In consistent with the current understanding of the mechanisms, whereby sMIC impairs host antitumor response, we demonstrated that our antibody neutralizing serum circulating sMIC restored NK cell homeostatic maintenance and function, restored NKG2D expression on CD8 T cells, and eliminated arginase 1⁺

myeloid suppressor cells systemically and in tumor microenvironment. Our data suggest that the immune suppression of sMIC in cancer patients could be reversed once sMIC is removed. Beyond overcoming the multiple immune suppressive effects of sMIC, very intriguingly, B10G5 therapy also enhanced antigen-specific CD8 T-cell responses and potentiated CD4 T cells to Th1 responses. More importantly, depletion of NK cells during therapy had more profound effect on CD4 T cells than on CD8 T cells. These findings suggest that the therapeutic effect on CD8 T cells is likely to be direct, whereas the effect on CD4 T cells is mediated through functional NK cells. The direct effect of anti-MIC antibody on CD8 T-cell responses may, in part, due to enhanced DC cross-presentation of antigens on MIC⁺ tumor cells through opsonization (22, 44, 45). This is also supported by our data demonstrating enhanced DC activation in tumor-dLN in response to anti-MIC therapy. How NK may regulate the response of CD4 T cells to anti-sMIC/MIC therapy is a very interesting question and warrants for further investigation.

Our data suggest that the therapeutic effect of B10G5 is conferred by complex mechanisms through multiple pathways. These may include: (i) reducing serum circulating sMIC to alleviate the global immune suppressive effect of sMIC in advanced diseases; (ii) effect of NK cell-mediated ADCC and/or enhanced immune synapse formation to enhance NKG2D-mediated interaction of NK cells with surface MIC⁺-tumor cells in less advanced diseases; (iii) enhanced DC presentation of antigens on MIC⁺ tumors; (iv)

potential complex formation of sMIC/B10G5 and subsequent immune stimulatory effect; (v) enhanced NK-DC cross-talk to better prime the adoptive immune responses. The impact of each mechanism on the therapeutic outcome warrants future investigation.

It is intriguing that antibody targeting sMIC therapy elicit a systemic cytokine and chemokine "storm," but with no detectable autoimmune toxicity. Notably, therapy not only induced high serum levels of antitumor cytokines, such as IL2, IFN γ , IL9, IL12, IL17, but also induced cytokines that regulates immune tolerance, such as IL4, IL10, and IL13. The balanced induction of immune active and immune tolerance cytokines may explain the absence of systemic autoimmune cytotoxicity. Given that MIC is a tumor-specific target, the absence of systemic autoimmunity may be reasonably expected.

In conclusion, with a "humanized" genetic engineered mouse model that recapitulate the dynamic interaction of human NKG2D ligand MIC with tumor progression, we demonstrate that an antibody neutralizing sMIC effectively induced regression of primary tumors and eliminated metastasis in advanced MIC⁺ malignancy. We further demonstrated that the mechanism of tumor suppression and clearance was conferred through restoring NK cell homeostatic maintenance and function, overcoming CD8 T-cell tolerance to tumor antigen, and heightening CD4 T cells to Th1 responses, and priming DCs for enhanced antigen presentation and tumor microenvironment to be more immune reactive. Furthermore, we demonstrate a critical role of NK cells in potentiating adaptive immune responses against tumors. Collectively, our study provided the first-in-field preclinical evidence demonstrating that an antibody neutralizing sMIC can reset and revamp endogenous antitumor responses to effectuate elimination of MIC⁺ malignancies. Our findings are highly translatable to clinics to treat MIC⁺ cancers with antibodies to neutralize sMIC. Conceptu-

ally, given the global overturning of endogenous antitumor responses induced by the sMIC-neutralizing antibody, sMIC may be considered as a tumor-specific immune checkpoint molecule.

Disclosure of Potential Conflicts of Interest

No potential conflicts of interest were disclosed.

Authors' Contributions

Conception and design: S. Lu, D. Liu, J.D. Wu

Development of methodology: S. Lu, G. Li, J.D. Wu

Acquisition of data (provided animals, acquired and managed patients, provided facilities, etc.): S. Lu, J. Zhang, D. Liu, J.D. Wu

Analysis and interpretation of data (e.g., statistical analysis, biostatistics, computational analysis): S. Lu, J. Zhang, G. Li, K.F. Staveley-O'Carroll, Z. Li, J.D. Wu

Writing, review, and/or revision of the manuscript: S. Lu, G. Li, K.F. Staveley-O'Carroll, J.D. Wu

Administrative, technical, or material support (i.e., reporting or organizing data, constructing databases): S. Lu, D. Liu, G. Li, K.F. Staveley-O'Carroll, J.D. Wu

Study supervision: K.F. Staveley-O'Carroll, J.D. Wu

Other (oversaw collaboration): J.D. Wu

Grant Support

This work was supported by NIH-NCI grant 1R01CA149405 and A. David Mazzone—Prostate Cancer Foundation Challenge Award (to J. Wu) and, in part, supported by the Flow Cytometry Core Facility Shared Resource, Hollings Cancer Center, Medical University of South Carolina (P30 CA138313).

The costs of publication of this article were defrayed in part by the payment of page charges. This article must therefore be hereby marked *advertisement* in accordance with 18 U.S.C. Section 1734 solely to indicate this fact.

Received April 5, 2015; revised June 4, 2015; accepted June 12, 2015; published OnlineFirst June 23, 2015.

References

- Gasser S, Orsulic S, Brown EJ, Raulet DH. The DNA damage pathway regulates innate immune system ligands of the NKG2D receptor. *Nature* 2005;436:1186–90.
- Groh V, Bahram S, Bauer S, Herman A, Beauchamp M, Spies T. Cell stress-regulated human major histocompatibility complex class I gene expressed in gastrointestinal epithelium. *Proc Natl Acad Sci U S A* 1996;93:12445–50.
- Gasser S, Raulet D. The DNA damage response, immunity and cancer. *Semin Cancer Biol* 2006;16:344–7.
- Raulet DH. Roles of the NKG2D immunoreceptor and its ligands. *Nat Rev Immunol* 2003;3:781–90.
- Diefenbach A, Jensen ER, Jamieson AM, Raulet DH. Rae1 and H60 ligands of the NKG2D receptor stimulate tumour immunity. *Nature* 2001;413:165–71.
- Maasho K, Opoku-Anane J, Marusina AI, Coligan JE, Borrego F. NKG2D is a costimulatory receptor for human naive CD8⁺ T cells. *J Immunol* 2005;174:4480–4.
- Liu G, Lu S, Wang X, Page ST, Higano CS, Plymate SR, et al. Perturbation of NK cell peripheral homeostasis accelerates prostate carcinoma metastasis. *J Clin Invest* 2013;123:4410–22.
- Fang L, Gong J, Wang Y, Liu R, Li Z, Wang Z, et al. MICA/B expression is inhibited by unfolded protein response and associated with poor prognosis in human hepatocellular carcinoma. *J Exp Clin Cancer Res* 2014;33:76.
- Chitadze G, Bhat J, Lettau M, Janssen O, Kabelitz D. Generation of soluble NKG2D ligands: proteolytic cleavage, exosome secretion and functional implications. *Scand J Immunol* 2013;78:120–9.
- Salih HR, Holdenrieder S, Steinle A. Soluble NKG2D ligands: prevalence, release, and functional impact. *Front Biosci* 2008;13:3448–56.
- Nausch N, Cerwenka A. NKG2D ligands in tumor immunity. *Oncogene* 2008;27:5944–58.
- Gang Xiao XW, Jun Sheng, Shengjun Lu, Xuezhong Yu, Jennifer D Wu. Soluble NKG2D ligand promotes MDSC expansion and skews macrophage to the alternatively activated phenotype. *J Hematol Oncol* 2015;8:13.
- Spear P, Wu MR, Sentman ML, Sentman CL. NKG2D ligands as therapeutic targets. *Cancer Immunol* 2013;13:8.
- Ullrich E, Koch J, Cerwenka A, Steinle A. New prospects on the NKG2D/NKG2DL system for oncology. *Oncoimmunology* 2013;2:e26097.
- Raulet DH, Gasser S, Gowen BG, Deng W, Jung H. Regulation of ligands for the NKG2D activating receptor. *Annu Rev Immunol* 2013;31:413–41.
- Groh V, Wu J, Yee C, Spies T. Tumour-derived soluble MIC ligands impair expression of NKG2D and T-cell activation. *Nature* 2002;419:734–8.
- Wu JD, Higgins LM, Steinle A, Cosman D, Haugk K, Plymate SR. Prevalent expression of the immunostimulatory MHC class I chain-related molecule is counteracted by shedding in prostate cancer. *J Clin Invest* 2004;114:560–8.
- Dobrovina ES, Dobrovina MM, Vider E, Sisson RB, O'Reilly RJ, Dupont B, et al. Evasion from NK cell immunity by MHC class I chain-related molecules expressing colon adenocarcinoma. *J Immunol* 2003;171:6891–9.

Lu et al.

19. Marten A, von Lilienfeld-Toal M, Buchler MW, Schmidt J. Soluble MIC is elevated in the serum of patients with pancreatic carcinoma diminishing gammadelta T cell cytotoxicity. *Int J Cancer* 2006;119:2359–65.
20. Holdenrieder S, Stieber P, Peterfi A, Nagel D, Steinle A, Salih HR. Soluble MICB in malignant diseases: analysis of diagnostic significance and correlation with soluble MICA. *Cancer Immunol Immunother* 2006;55:1584–9.
21. Holdenrieder S, Stieber P, Peterfi A, Nagel D, Steinle A, Salih HR. Soluble MICA in malignant diseases. *Int J Cancer* 2006;118:684–7.
22. Jinushi M, Vanneman M, Munshi NC, Tai YT, Prabhala RH, Ritz J, et al. MHC class I chain-related protein A antibodies and shedding are associated with the progression of multiple myeloma. *Proc Natl Acad Sci U S A* 2008;105:1285–90.
23. Wu JD, Higgins LM, Steinle A, Cosman D, Haugk K, Plymate SR. Prevalent expression of the immunostimulatory MHC class I chain-related molecule is counteracted by shedding in prostate cancer. *J Clin Invest* 2004;114:560–8.
24. Deng W, Gowen BG, Zhang L, Wang L, Lau S, Iannello A, et al. A shed NKG2D ligand that promotes natural killer cell activation and tumor rejection. *Science* 2015;348:136–9.
25. Strong RK. Asymmetric ligand recognition by the activating natural killer cell receptor NKG2D, a symmetric homodimer. *Mol Immunol* 2002;38:1029–37.
26. Staveley-O'Carroll K, Schell TD, Jimenez M, Mylin LM, Tevethia MJ, Schoenberger SP, et al. *In vivo* ligation of CD40 enhances priming against the endogenous tumor antigen and promotes CD8⁺ T cell effector function in SV40 T antigen transgenic mice. *J Immunol* 2003;171:697–707.
27. Wu J. NKG2D Ligands in cancer immunotherapy: target or not? *Austin J Clin Immunol* 2014;1:2.
28. Marcu M, Radu E, Sajin M. Neuroendocrine transdifferentiation of prostate carcinoma cells and its prognostic significance. *Rom J Morphol Embryol* 2010;51:7–12.
29. Sun Y, Niu J, Huang J. Neuroendocrine differentiation in prostate cancer. *Am J Transl Res* 2009;1:148–62.
30. Ishigami S, Natsugoe S, Tokuda K, Nakajo A, Che X, Iwashige H, et al. Prognostic value of intratumoral natural killer cells in gastric carcinoma. *Cancer* 2000;88:577–83.
31. Coca S, Perez-Piqueras J, Martinez D, Colmenarejo A, Saez MA, Vallejo C, et al. The prognostic significance of intratumoral natural killer cells in patients with colorectal carcinoma. *Cancer* 1997;79:2320–8.
32. Desbois M, Rusakiewicz S, Locher C, Zitvogel L, Chaput N. Natural killer cells in non-hematopoietic malignancies. *Front Immunol* 2012;3:395.
33. Takanami I, Takeuchi K, Giga M. The prognostic value of natural killer cell infiltration in resected pulmonary adenocarcinoma. *J Thorac Cardiovasc Surg* 2001;121:1058–63.
34. Villegas FR, Coca S, Villarrubia VG, Jimenez R, Chillon MJ, Jareno J, et al. Prognostic significance of tumor infiltrating natural killer cells subset CD57 in patients with squamous cell lung cancer. *Lung Cancer* 2002;35:23–8.
35. Nagaraj S, Gabrilovich DI. Tumor escape mechanism governed by myeloid-derived suppressor cells. *Cancer Res* 2008;68:2561–3.
36. Rodriguez PC, Ernstoff MS, Hernandez C, Atkins M, Zabaleta J, Sierra R, et al. Arginase I-producing myeloid-derived suppressor cells in renal cell carcinoma are a subpopulation of activated granulocytes. *Cancer Res* 2009;69:1553–60.
37. Martinez FO, Sica A, Mantovani A, Locati M. Macrophage activation and polarization. *Front Biosci* 2008;13:453–61.
38. Martinez FO, Helming L, Gordon S. Alternative activation of macrophages: an immunologic functional perspective. *Annu Rev Immunol* 2009;27:451–83.
39. Jinushi M, Takehara T, Tatsumi T, Hiramatsu N, Sakamori R, Yamaguchi S, et al. Impairment of natural killer cell and dendritic cell functions by the soluble form of MHC class I-related chain A in advanced human hepatocellular carcinomas. *J Hepatol* 2005;43:1013–20.
40. Deeb KK, Michalowska AM, Yoon CY, Krummey SM, Hoenerhoff MJ, Kavanaugh C, et al. Identification of an integrated SV40 T/t-antigen cancer signature in aggressive human breast, prostate, and lung carcinomas with poor prognosis. *Cancer Res* 2007;67:8065–80.
41. Zheng X, Gao JX, Zhang H, Geiger TL, Liu Y, Zheng P. Clonal deletion of simian virus 40 large T antigen-specific T cells in the transgenic adenocarcinoma of mouse prostate mice: an important role for clonal deletion in shaping the repertoire of T cells specific for antigens overexpressed in solid tumors. *J Immunol* 2002;169:4761–9.
42. Bai A, Higham E, Eisen HN, Witttrup KD, Chen J. Rapid tolerization of virus-activated tumor-specific CD8⁺ T cells in prostate tumors of TRAMP mice. *Proc Natl Acad Sci U S A* 2008;105:13003–8.
43. Shafer-Weaver KA, Watkins SK, Anderson MJ, Draper LJ, Malyguine A, Alvord WG, et al. Immunity to murine prostatic tumors: continuous provision of T-cell help prevents CD8 T-cell tolerance and activates tumor-infiltrating dendritic cells. *Cancer Res* 2009;69:6256–64.
44. Groh V, Li YQ, Cioca D, Hunder NN, Wang W, Riddell SR, et al. Efficient cross-priming of tumor antigen-specific T cells by dendritic cells sensitized with diverse anti-MICA opsonized tumor cells. *Proc Natl Acad Sci U S A* 2005;102:6461–6.
45. Jinushi M, Hodi FS, Dranoff G. Therapy-induced antibodies to MHC class I chain-related protein A antagonize immune suppression and stimulate antitumor cytotoxicity. *Proc Natl Acad Sci U S A* 2006;103:9190–5.
46. Baragano Raneros A, Suarez-Alvarez B, Lopez-Larrea C. Secretory pathways generating immunosuppressive NKG2D ligands: new targets for therapeutic intervention. *Oncoimmunology* 2014;3:e28497.
47. Kaiser BK, Yim D, Chow IT, Gonzalez S, Dai Z, Mann HH, et al. Disulphide-isomerase-enabled shedding of tumour-associated NKG2D ligands. *Nature* 2007;447:482–6.
48. Fonseca C, Soiffer R, Ho V, Vanneman M, Jinushi M, Ritz J, et al. Protein disulfide isomerases are antibody targets during immune-mediated tumor destruction. *Blood* 2009;113:1681–8.
49. Waldhauer I, Goehlsdorf D, Gieseke F, Weinschenk T, Wittenbrink M, Ludwig A, et al. Tumor-associated MICA is shed by ADAM proteases. *Cancer Res* 2008;68:6368–76.
50. Liu G, Atteridge CL, Wang X, Lundgren AD, Wu JD. The membrane type matrix metalloproteinase MMP14 mediates constitutive shedding of MHC class I chain-related molecule A independent of A disintegrin and metalloproteinases. *J Immunol* 2010;184:3346–50.

Clinical Cancer Research

Nonblocking Monoclonal Antibody Targeting Soluble MIC Revamps Endogenous Innate and Adaptive Antitumor Responses and Eliminates Primary and Metastatic Tumors

Shengjun Lu, Jinyu Zhang, Dai Liu, et al.

Clin Cancer Res 2015;21:4819-4830. Published OnlineFirst June 23, 2015.

Updated version Access the most recent version of this article at:
doi:[10.1158/1078-0432.CCR-15-0845](https://doi.org/10.1158/1078-0432.CCR-15-0845)

Supplementary Material Access the most recent supplemental material at:
<http://clincancerres.aacrjournals.org/content/suppl/2015/06/24/1078-0432.CCR-15-0845.DC1.html>

Cited articles This article cites 50 articles, 18 of which you can access for free at:
<http://clincancerres.aacrjournals.org/content/21/21/4819.full.html#ref-list-1>

E-mail alerts [Sign up to receive free email-alerts](#) related to this article or journal.

Reprints and Subscriptions To order reprints of this article or to subscribe to the journal, contact the AACR Publications Department at pubs@aacr.org.

Permissions To request permission to re-use all or part of this article, contact the AACR Publications Department at permissions@aacr.org.